Photodynamic therapy-induced nitric oxide production in neuronal and glial cells

Vera D. Kovaleva
Anatoly B. Uzdensky

SPIE.

Photodynamic therapy-induced nitric oxide production in neuronal and glial cells

Vera D. Kovaleva and Anatoly B. Uzdensky*
Southern Federal University, Laboratory of Molecular Neurobiology, Academy of Biology and Biotechnology, Stachky Avenue 194/1, 344090 Rostov-on-Don, Russia

Abstract. Nitric oxide (NO) has been recently demonstrated to enhance apoptosis of glial cells induced by photodynamic therapy (PDT), but to protect glial cells from PDT-induced necrosis in the crayfish stretch receptor, a simple neuroglial preparation that consists of a single mechanosensory neuron enveloped by satellite glial cells. We used the NO-sensitive fluorescent probe 4,5-diaminofluorescein diacetate to study the distribution and dynamics of PDT-induced NO production in the mechanosensory neuron and surrounding glial cells. The NO production in the glial envelope was higher than in the neuronal soma axon and dendrites both in control and in experimental conditions. In dark NO generator, DEA NONOate or NO synthase substrate L-arginine hydrochloride significantly increased the NO level in glial cells, whereas NO scavenger 2-Phenyl-4,4,5,5-tetramethylimidazoline-1-oxyl 3-oxide (PTIO) or inhibitors of NO synthase L-NG-nitro arginine methyl ester and Nω-nitro-L-arginine decreased it. PDT induced the transient increase in NO production with a maximum at 4 to 7 min after the irradiation start followed by its inhibition at 10 to 40 min. We suggested that PDT stimulated neuronal rather than inducible NO synthase isoform in glial cells, and the produced NO could mediate PDT-induced apoptosis. © *2016 Society of Photo-Optical Instrumentation Engineers (SPIE)* [DOI: 10.1117/1.JBO.21.10.105005]

Keywords: photodynamic therapy; nitric oxide; neuron; glia.

Paper 160369RR received Jun. 6, 2016; accepted for publication Oct. 5, 2016; published online Oct. 26, 2016.

1 Introduction

Photodynamic therapy (PDT) is based on light-induced death of cells stained with a photosensitizing dye in the presence of oxygen. Photoexcitation of the sensitizer molecules leads to generation of singlet oxygen and other reactive oxygen species that induce oxidative stress and kill the cells. PDT is used to treat cancer, including brain tumors.[1–3] Not only tumor cells, but also normal nerve and glial cells are damaged during brain PDT. Thus, the study of signaling mechanisms regulating photodynamic damage or protection of normal neurons and glial cells are of importance.[4] However, in the mammalian brain, numerous neurons interact with hundreds of other neurons. It is difficult to identify them and determine which glial cells interact with a given neuron. The use of a simpler neuroglial system such as the crayfish stretch receptor (CSR) that consists of a single mechanoreceptor neuron surrounded by the glial envelope[5,6] is preferable. It has been used as a simple but informative experimental model in the studies of signaling mechanisms of photodynamic effect on neurons and glial cells.[4,7–9]

Nitric oxide (NO) is a second messenger, involved in the regulation of various cellular functions. It participates in neurotransmission, cell responses to stress, and neurodegeneration.[10,11] PDT has been shown to induce NO production in different cell lines.[12–14] Some authors have also demonstrated the involvement of NO in PDT-induced apoptosis.[12,15] On the other hand, it was shown that NO can protect tumor cells from PDT-induced death either through inhibition of lipid peroxidation in the cellular membranes[16,17] or through cGMP-dependent signaling pathway.[18] Some authors did not find any correlations between NO

production and PDT-induced cell damage.[19] Thus, the role of NO in cell death is not clearly understood yet. The role of NO in PDT-induced death of neuronal and glial cells is also insufficiently studied. As recently shown, NO enhances PDT-induced apoptosis of glial cells in the CSR. At the same time, it protects crayfish glial cells from PDT-induced necrosis.[7]

The dynamics of NO production during PDT has not been well examined. Some authors studied NO production at different post-PDT time points, but not during the treatment.[14] Another important problem is the mechanism of neuroglial interactions under stress conditions. The crayfish mechanoreceptor neuron is known to protect satellite glial cells from PDT-induced apoptosis but not necrosis.[20] These neuroglial interactions may be mediated by a intercellular signaling messenger such as neurotrophic factors.[21,22] or NO. Is NO involved in the neuroglial interactions in the photosensitized CSR? What is the source of NO, the neuron, or glial cells? What is the dynamics of NO production? In this work, we addressed these questions using the NO-sensitive fluorescence probe 4,5-diaminofluorescein diacetate that provides NO visualization and accurate and fast measurement of the dynamics of its production.

2 Materials and Methods

The following chemicals were used in this work: the NO-sensitive fluorescent probe 4,5-diaminofluorescein diacetate (DAF-2DA), NO generator DEA NONOate (25 μM), NO synthase (NOS) substrate L-arginine hydrochloride (L-arg HCl) (500 μM), NO scavenger PTIO (500 μM), nonspecific NO synthase (NOS) inhibitors L-NG-nitro arginine methyl ester (L-NAME) (1 mM) and Nω-nitro-L-arginine (L-NNA) (1 mM), inhibitor of the

*Address all correspondence to: Anatoly B. Uzdensky, E-mail: auzd@yandex .ru
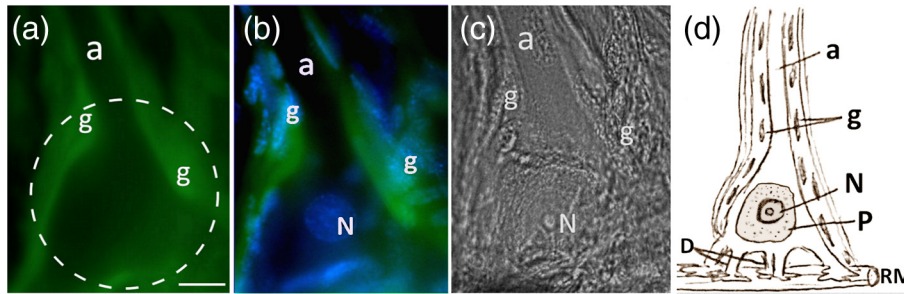
Fig. 1 The distribution of NO in the mechanoreceptor neuron and satellite glia of the CSR. (a) Fluorescent image of the CSR stained with NO-sensitive fluorescent probe DAF-2DA; (b) double fluorochrome staining of the same preparation with NO probe DAF-2DA (green) and Hoechst-33342 that visualizes the nuclei of neurons and glial cells (blue); (c) brightfield image of same stretch receptor; and (d) the scheme of the CSR morphology. a, axon; D, dendrites; g, glial cells; N, neuronal nucleus; P, perikaryon; RM, receptor muscle. Scale bar 15 μm.

inducible NOS isoform (iNOS) 5-methylisothiourea hemisulfate (SMT) (500 μM, 1 mM, 10 mM), and the fluorescent dye Hoechst-33342. All chemicals were purchased from Sigma-Aldrich Rus (Moscow, Russia). Photosensitizer photosens, a mixture of sulphonated alumophthalocyanines AlPcS$_n$, where mean $n = 3.1$, was obtained from NIOPIK (Moscow, Russia).

The abdominal stretch receptors of the crayfish *Astacus leptodactylus* that contain single sensory neurons, surrounded by the multilayer glial envelope,[6] were isolated as described in Ref. 5. The isolated receptors were placed into the chamber filled with van Harreveld's saline for cold-blooded animals (mM: NaCl, 205; KCl, 5.4; NaHCO$_3$, 0.24; MgCl$_2$, 5.4; CaCl$_2$, 13.5; pH 7.2 to 7.4). Spikes were recorded extracellularly from axons by glass suction electrodes and processed by a personal computer using the home-made software providing continuous firing monitoring and registration of firing rates. The initial firing level was set at 6 to 10 Hz by application of the appropriate receptor muscle extension.

The NO production was examined using the fluorescent probe 4,5-diaminofluorescein diacetate (DAF-2DA). This cell-permeable and highly sensitive NO probe forms intensely fluorescing 4,5-diaminofluorescein triazole (DAF-2T) upon direct reaction with NO inside the cell.[23] This technique has been used to study the real-time changes in intracellular NO level in various conditions in different animal models, including invertebrates.[24,25] After 30-min control recording of the neuronal activity, the preparations were incubated 60 min in the saline containing DAF-2DA (1:500). Then the samples were washed out five times with the dye-free saline to remove the excess of the dye. Photosens (10 nM) was added into the chamber, and after a 30-min incubation, the preparations were irradiated by the diode laser (670 nm, 0.8 W/cm^2, 3-mm beam diameter). Then the stretch receptor preparations were replaced from the electrophysiological apparatus to the Axio Lab. A1 microscope (Carl Zeiss), equipped with the AxioCam ERc 5s camera, which registered the fluorescence of DAF-2DA before PDT and 1, 4, 7, 10, 15, 20, 25, 30, and 40 min during PDT. The images were acquired with ZEN 2012 (Carl Zeiss) software on the personal computer (Intel Core i3, 3.10 GHz, RAM 4 Gb, Windows 7 Enterprise 64 bit) and processed using Image-Pro Plus Version 6.0 (Media Cybernetics) software. The mean fluorescence intensity was measured within the circle ($\varnothing$100 μm) around the neuronal soma [Fig. 1(a)] that contained the neuronal nucleus and 30 to 40 nuclei of surrounding glial cells. It was then normalized relatively to the fluorescence intensity of the distant stretch receptor region, where the fluorescence intensity did not change. Application of NO generator DEA NONOate (25 μM), NOS substrate L-arginine hydrochloride (500 μM), NO scavenger PTIO (500 μM), NOS inhibitors L-NAME (1 mM), L-NNA (1 mM), and iNOS inhibitor SMT (500 μM, 1 mM, 10 mM) were used as a positive or negative control of NO production. All experiments were performed at 24 $\pm$ 2°C. Statistical evaluation of the difference between independent experimental groups was performed using one-way ANOVA. Results are presented as mean $\pm$ SEM.

3 Results

The morphology of the isolated stretch receptor in the control preparations is shown in Figure 1. The dendrites of the single mechanoreceptor neuron are known to attach to the receptor muscle and ramify between muscle fibers, whereas the axon goes to the ventral cord ganglion.[5,6] Satellite glial cells form the roulette-like envelope around the neuronal soma and processes.[6] Due to such morphology, the cytoplasm of separate glial cells cannot be distinguished at the optical level, but the nuclei of

Table 1 The mean fluorescence intensity of DAF-2DA (relative units $\pm$ SEM) in glial cells, neuronal soma, receptor muscle, and axon at different time points during PDT ($n = 9$).

t (min)	Neuronal soma	Axon	Glial cells	Dendrites
0	13.5 $\pm$ 1.1	12.2 $\pm$ 0.9	39.8 $\pm$ 0.5	22.5 $\pm$ 1.7
1	14.2 $\pm$ 1.4	14.2 $\pm$ 1.2	42.3 $\pm$ 0.6	31.5 $\pm$ 3.2
4	15.8 $\pm$ 2.1	16.5 $\pm$ 2.2	59.3 $\pm$ 2.1	47.5 $\pm$ 2.8
7	16.3 $\pm$ 0.9	16.9 $\pm$ 1.9	60.6 $\pm$ 1.6	48.3 $\pm$ 3.2
10	12.6 $\pm$ 1.8	11.3 $\pm$ 2.5	33.2 $\pm$ 1.4	21.6 $\pm$ 1.3
15	9.2 $\pm$ 0.9	11.5 $\pm$ 3.3	20.8 $\pm$ 2.6	18.9 $\pm$ 3.6
20	8.5 $\pm$ 1.8	10.8 $\pm$ 1.6	19.8 $\pm$ 2.4	18.2 $\pm$ 2
25	8.8 $\pm$ 1.6	10.5 $\pm$ 2.1	19.5 $\pm$ 3.2	17.5 $\pm$ 3.4
30	11.4 $\pm$ 2.3	11.3 $\pm$ 3.7	16.5 $\pm$ 1.9	17 $\pm$ 2.6
40	10.8 $\pm$ 2	11 $\pm$ 1.9	16.7 $\pm$ 2.5	17.3 $\pm$ 2.3

different glial cells fluorochromed by Hoechst-33342 are clearly seen in Fig. 1(b) and Ref. 6.

The distribution and dynamics of DAF-2DA fluorescence that displays the NO location and production in the CSR preparation is shown in Figs. 1(a) and 1(b). The mean fluorescence intensity in control glial cells before PDT was 39.8 ± 0.5 relative units (Table 1, at $t = 0$). The mean levels of DAF-2DA fluorescence in the neuronal axon, soma, and dendrites [points a, s, and d in Fig. 2(a)] were 3.3, 2.9, and 1.8 times lower than in the glial envelope (point g), respectively (Table 1, at $t = 0$).

The glial envelope around the sensory neuron can be observed in the overlay of DAF-2DA fluorescence image [Fig. 1(a)] and the image of Hoechst-33342 staining, which shows the nuclei of glial cells and neurons [Fig. 1(b)].

To check if the changes in the mean intensity of DAF-2DA fluorescence were due to the changes in NO level, we applied NO generator DEA NONOate (25 μM) or NOS substrate L-arginine hydrochloride (500 μM), NO scavenger PTIO (500 μM) and NOS-inhibitors L-NAME (1 mM), L-NNA (1 mM), and SMT (500 μM, 1 mM, 10 mM) in the absence of photosensitizer (Table 2). All these modulators did not change neuronal activity during the experiment.

DEA NONOate, applied after DAF-2DA, increased the mean intensity of DAF-2DA fluorescence [measured within the circle shown in Fig. 1(a)] by 1.4 and 2.3 times for 5 and 10 min, respectively (Table 2). During next 50 min, it gradually decreased by 1.7 times as compared with the maximal level and did not change during the next 60 min. L-arginine increased the mean intensity of DAF-2DA fluorescence by 1.9 times for 60 min. This level was maintained during the next 3 h, and then slightly decreased (Table 2).

NO scavenger PTIO, applied 1 h before DAF-2DA, almost completely blocked the DAF-2DA fluorescence (Table 2). The nonspecific NOS inhibitors L-NAME and L-NNA, applied 1 h
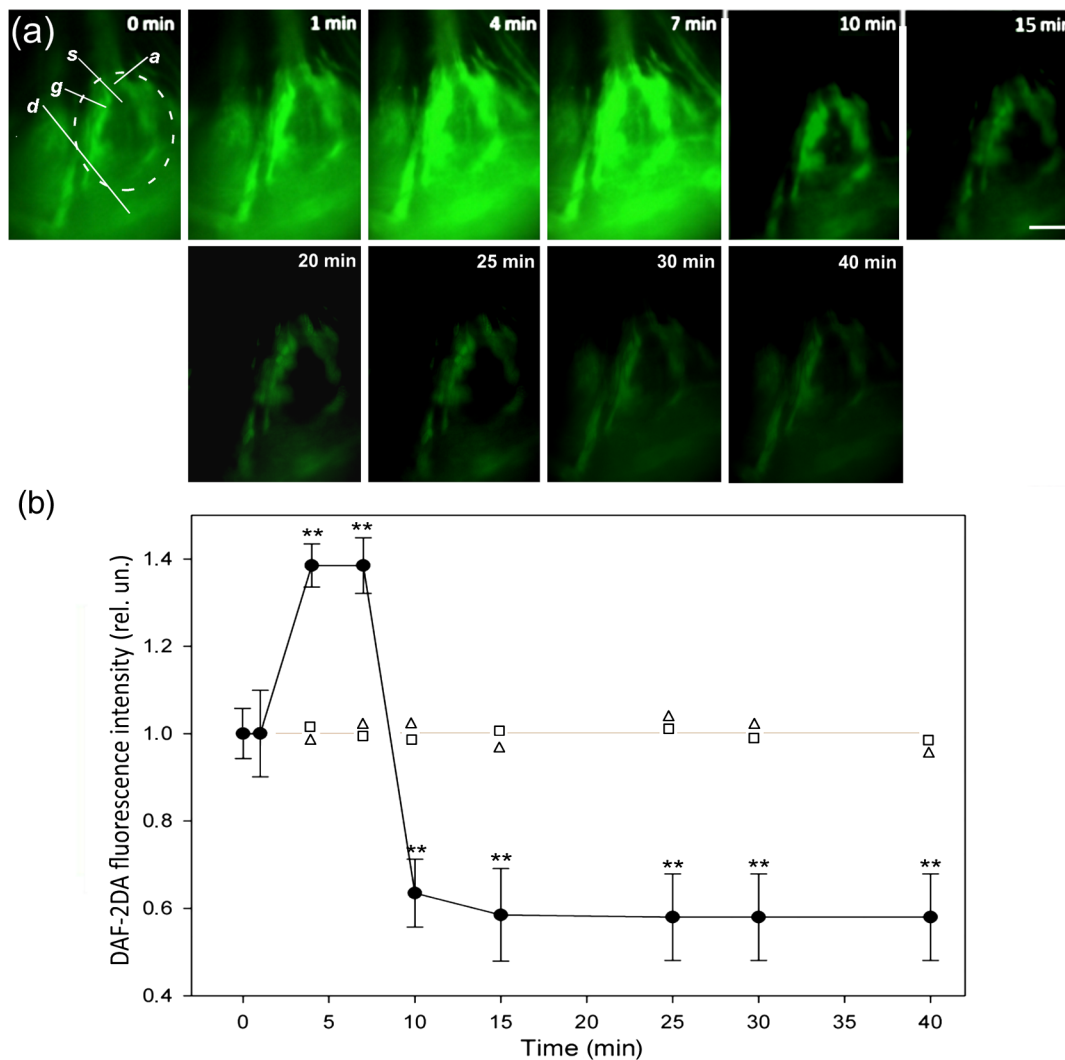
Fig. 2 The dynamics of NO production in the isolated CSR during PDT evaluated with NO-sensitive fluorescence probe DAF-2DA. (a) DAF-2DA fluorescence in the CSR before and at different time intervals during PDT. The dashed circle indicates the region of interest. Points a, s, d, and g show the regions of local measurements of DAF-2A fluorescence in small squares (5 × 5 μm²) within the neuronal axon, soma, dendrite region, and in glial cells, respectively. (b) The dynamics of the mean fluorescence intensity of DAF-2DA: squares, laser only treatment ($n = 6$); triangles, photosensitizer only treatment ($n = 6$); circles, PDT effect ($n = 9$). Asterisks indicate the significant difference from initial fluorescence level (**$p < 0.01$). Scale bar 30 μm.

Table 2 The changes in the mean fluorescence intensity of DAF-2DA in the presence of NO-generator DEA NONOate (25 μM), NOS substrate L-arginine hydrochloride (500 μM), NO scavenger PTIO (500 μM), nNOS inhibitors L-NAME (1 mM), L-NNA (1 mM), and SMT (500 μM) in the absence of PDT relatively to the initial fluorescence level ($t = 0$). Significant difference from the mean fluorescence intensity in the control group: **$p < 0.01$ or ***$p < 0.001$. The number of experiments is indicated in brackets.

Modulator	t (min)	Mean fluorescence intensity (rel. un.)
Control	0	26.7 ± 0.4 (9)
NONOate (25 μM)	5	37.6 ± 1.1 (8)**
	10	62.6 ± 0.6 (8)**
	20	55.7 ± 0.7 (8)**
	30	53.2 ± 0.3 (8)**
	40	39.2 ± 0.9 (8)**
	60	36.8 ± 1.1 (8)**
	120	36.2 ± 1.5 (8)**
L-arginine (500 μM)	10	28.2 ± 0.6 (7)
	60	51.7 ± 1.6 (7)***
	120	51.7 ± 1.6 (7)***
	180	51.6 ± 1.6 (7)***
	240	42.6 ± 1.2 (7)**
PTIO (500 μM)	60	1.2 ± 0.3 (7)***
L-NAME (1 mM)	60	14.8 ± 1.2 (7)***
L-NNA (1 mM)	60	15.5 ± 1.5 (7)***
SMT (500 μM)	60	25.4 ± 2 (6)

before DAF-2DA, decreased the mean intensity of DAF-2DA fluorescence by 1.7 to 1.8 times (Table 2), whereas iNOS inhibitor SMT did not influence DAF-2DA fluorescence.

The dynamics of DAF-2DA fluorescence in the CSR under laser irradiation, or photosensitizer application, or under their combined action (PDT) are shown in Fig. 2. Laser irradiation or photosensitizer application acting separately did not influence the mean intensity of DAF-2DA fluorescence in the CSR [Fig. 2(b)].

PDT transiently increased DAF-2DA fluorescence by 1.4 times at 4 to 7 min after PDT start [Figs. 2(a) and 2(b)]. However, at 10 min, the mean intensity of DAF-2DA fluorescence decreased by 40% relatively to the initial level and did not change further during next 30 min [Fig. 2(b)].

We also compared the dynamics of PDT-induced NO production in different parts of the CSR: neuronal axon, soma, dendrite region, and glial envelope (points a, s, d, and g, respectively, shown in [Fig. 2(a)]. In this experiment, we measured DAF-2A fluorescence in small squares (5×5 μm^2) within these regions. The distribution of NO during PDT was similar to that in the control preparations. The highest DAF-2A fluorescence

was observed in the glial envelope around the neuronal body [Fig. 2(a) and Table 1]. The redistribution of the NO probe fluorescence was not observed.

4 Discussion

The presented experiments confirmed the specificity of DAF-2DA to detect the intracellular NO level[23–25] in crayfish neurons and glial cells. DAF-2DA fluorescence increased in the presence of the exogenous (DEA NONOate), or endogenous (L-arginine hydrochloride) NO generators, or decreased under application of NO scavenger (PTIO), or NO synthase inhibitors (L-NAME, L-NNA). The separate application of the photosensitizer or laser irradiation did not influence DAF-2DA fluorescence. Although some authors assume that changes in the DAF-2DA fluorescence can be associated not only with NO production,[26] it is commonly accepted that the DAF probes have a detection limit for NO as low as 5 nM and show no fluorescence in the presence of various interferents such as NO_2^-, NO_3^-, H_2O_2, and peroxynitrite ($ONOO^-$).[23,27] It should be noted that we observed the delay in the increase of DAF-2DA fluorescence in the presence of NONOate or L-arginine: 10 and 60 min, respectively, and then a slow decrease (Table 2). This nonlinear kinetics should be taken into account in the prolonged NO measurements. Nevertheless, DAF-2DA fluorescence is a relevant method for registration of NO production dynamics, although quick measurements do not reach the maximal NO sensitivity.

Both inducible and neuronal isoforms of NO synthase (iNOS and nNOS, respectively) have been found in neurons and glial cells.[28,29] These were involved in the PDT-induced death of crayfish neurons and glia,[7] as well as in death of other cells.[29,30] NO scavenger PTIO suppressed DAF-2DA fluorescence almost completely, whereas nonselective NOS inhibitors, L-NAME and L-NNA, reduced it only by 1.7 to 1.8 times. One can hypothesize the presence of additional NO sources, other than nNOS and iNOS, which are not affected by L-NAME and L-NNA. It may be mitochondrial NO synthase incorporated into the inner mitochondrial membrane and performing some functions of neuronal NOS.[31] PTIO can also scavenge NO, formed during the nonenzymatic destruction of nitrites or nitrates. These inert anions can be important alternative source of NO, in particular in the hypoxic state.[32]

In our experiments, PDT rapidly increased for 4 min the NO level which was followed by its decrease after 7 min (Fig. 2). Similarly, the transient activation of NO production in the cancer cell lines was followed by inhibition, possibly due to nNOS destruction by reactive oxygen species.[25] One can suggest that the fast PDT-induced increase in NO production in the CSR preparation could be due to activation of nNOS rather than iNOS. In fact, a 4-min interval is too short to express iNOS. Additionally, iNOS inhibitor SMT did not influence the NO level (Table 2). nNOS is known to be activated by intracellular Ca^{2+} and PDT rapidly increases the cytosolic Ca^{2+} level.[33,34] Finally, the correlation between the cytosolic calcium level and NO production during photodynamic treatment has been reported.[35,36]

We showed previously that NO mediates PDT-induced apoptosis of glial cells.[7] This raised the question: what is the source of NO in this neuroglial preparation, the neuron or glia? The present experiments showed that NO production was concentrated mainly in the glial envelope around the neuron soma, and, to a lesser extent, in the proximal dendrite zone. (However, in this location, we could not separate possible NO sources

between the proximal parts of dendrites, or the glial envelope, or both.) NO levels inside the neuronal soma, nucleus, and axon of the mechanoreceptor neuron were much lower. One can suggest that the proapoptotic effect of NO on the photosensitized crayfish glial cells observed in our previous work[7] was due to NO production in the glial cells rather than in the mechanoreceptor neuron. Additionally, taking into the account that the glial area of NO production was much higher than that in dendrites, one can suggest the glial envelope to be the main NO source. The increase of NO level in the beginning of PDT action could initiate the proapoptotic cascades in glial cells. As we showed previously, the neuronal soma protects satellite glial cells from PDT-induced apoptosis.[20] This function could be performed by intercellular messengers such as neurotrophic factors NGF and GDNF.[21,22] The role of another intercellular messenger NO was unknown. The present data showed that NO could be involved in neuroglial interactions during PDT. However, it played the proapoptotic rather than antiapoptotic role.[9] On the other hand, NO produced in the glial envelope could protect neurons from PDT-induced necrosis and impairment of neuronal activity.[7]

Acknowledgments

References

1. S. S. Stylli and A. H. Kaye, "Photodynamic therapy of cerebral glioma—a review. Part I. A biological basis," *J. Clin. Neurosci.* **13**, 615–625 (2006).
2. B. J. Quirk et al., "Photodynamic therapy (PDT) for malignant brain tumors–where do we stand?" *Photodiagn. Photodyn. Ther.* **12**, 530–544 (2015).
3. H. Kostron, "Photodynamic diagnosis and therapy and the brain," in *Photodynamic Therapy: Methods and Protocols, Methods in Molecular Biology*, C. J. Gomer, Ed., p. 635, Springer Science + Business Media, Berlin (2010).
4. A. B. Uzdensky, *Cellular and Molecular Mechanisms of Photodynamic Therapy*, Nauka, Sankt-Petersburg (2010).
5. E. Florey and E. Florey, "Microanatomy of the abdominal stretch receptors of the crayfish (Astacus fluviatilis L.)," *J. Gen. Physiol.* **39**, 69–85 (1955).
6. G. M. Fedorenko and A. B. Uzdensky, "Ultrastructure of neuroglial contacts in crayfish stretch receptor," *Cell Tissue Res.* **337**, 477–490 (2009).
7. V. D. Kovaleva et al., "Involvement of nitric oxide in photodynamic injury of neurons and glial cells," *Nitric Oxide* **29**, 46–52 (2013).
8. A. B. Uzdensky et al., "The response of neurons and glial cells of crayfish to photodynamic treatment: transcription factors and epigenetic regulation," *Biochem. Suppl. Ser. A* **9**, 329–336 (2015).
9. A. B. Uzdensky et al., "Protection of the crayfish mechanoreceptor neuron and glial cells from photooxidative injury by modulators of diverse signal transduction pathways," *Mol. Neurobiol.* **52**(2), 811–825 (2015).
10. S. Moncada and J. P. Bolanos, "Nitric oxide, cell bioenergetics and neurodegeneration," *J. Neurochem.* **97**, 1676–1689 (2006).
11. G. C. Brown, "Nitric oxide and neuronal death," *Nitric Oxide* **23**, 153–165 (2010).
12. S. Gupta, N. Ahmad, and H. Mukhtar, "Involvement of nitric oxide during phthalocyanine (Pc4) photodynamic therapy-mediated apoptosis," *Cancer Res.* **58**, 1785–1788 (1998).
13. S. Coutier et al., "Foscan (mTHPC) photosensitized macrophage activation: enhancement of phagocytosis, nitric oxide release and tumour necrosis factor-alpha-mediated cytolytic activity," *Br. J. Cancer* **81**, 37–42 (1999).
14. S. M. Ali and M. Olivo, "Nitric oxide mediated photo-induced cell death in human malignant cells," *Int. J. Oncol.* **22**, 751–756 (2003).
15. Z. Lu et al., "Mitochondrial reactive oxygen species and nitric oxide-mediated cancer cell apoptosis in 2- butylamino-2-demethoxyhypocrellin B photodynamic treatment," *Free Radical Biol. Med.* **41**, 1590–1605 (2006).
16. M. Niziolek, W. Korytowski, and A. W. Girotti, "Chain-breaking antioxidant and cytoprotective action of nitric oxide on photo photodynamically stressed tumor cells," *J. Photochem. Photobiol.* **78**, 262–270 (2003).
17. M. Niziolek, W. Korytowski, and A. W. Girotti, "Nitric oxide-induced resistance to lethal photooxidative damage in a breast tumor cell line," *Free Radic. Biol. Med.* **40**, 1323–1331 (2006).
18. E. R. Gomes et al., "Nitric oxide modulates tumor cell death induced by photodynamic therapy through a cGMP-dependent mechanism," *J. Photochem. Photobiol.* **76**, 423–430 (2002).
19. G. Di Venosa et al., "Sensitivity to ALA-PDT of cell lines with different nitric oxide production and resistance to NO cytotoxicity," *J. Photochem. Photobiol.* **80**, 195–202 (2005).
20. M. Kolosov and A. Uzdensky, "Crayfish mechanoreceptor neuron prevents photoinduced apoptosis of satellite glial cells," *Brain Res. Bull.* **69**, 495–500 (2006).
21. A. V. Lobanov and A. B. Uzdensky, "Protection of crayfish glial cells but not neurons from photodynamic Injury by nerve growth factor," *J. Mol. Neurosci.* **39**, 308–319 (2009).
22. A. B. Uzdensky et al., "Protection effect of GDNF and neurturin on photosensitized crayfish neurons and glial cells," *J. Mol. Neurosci.* **49**, 480–490 (2013).
23. H. Kojima et al., "Detection and imaging of nitric oxide with novel fluorescent indicators: diaminofluoresceins," *Anal. Chem.* **70**(13), 2446–2453 (1998).
24. X. Ye et al., "Production of nitric oxide within the aplysia californica nervous system," *ACS Chem. Neurosci.* **1**, 182–193 (2010).
25. R. Bhowmick and A. W. Girotti, "Rapid upregulation of cytoprotective nitric oxide in breast tumor cells subjected to a photodynamic therapy-like oxidative challenge," *Photochem. Photobiol.* **87**(2), 378–386 (2011).
26. C. Csonka et al., "Measurement of NO in biological samples," *Br. J. Pharmacol.* **172**, 1620–1632 (2015).
27. E. M. Hetrick and M. H. Schoenfisch, "Analytical chemistry of nitric oxide," *Annu. Rev. Anal. Chem.* **2**, 409–433 (2009).
28. S. Murphy et al., "Synthesis of nitric oxide in CNS glial cells," *Trends Neurosci.* **16**, 323–328 (1993).
29. K. J. Reeves, M. W. Reed, and N. J. Brown, "Is nitric oxide important in photodynamic therapy?" *J. Photochem. Photobiol.* **95**, 141–147 (2009).
30. R. Bhowmick and A. W. Girotti, "Cytoprotective induction of nitric oxide synthase in a cellular model of 5-aminolevulinic acid-based photodynamic therapy," *Free Rad. Biol. Med.* **48**, 1296–1301 (2010).
31. P. V. Finocchietto et al., "Mitochondrial nitric oxide synthase: a masterpiece of metabolic adaptation, cell growth, transformation, and death," *Exp. Biol. Med.* **234**(9), 1020–1028 (2009).
32. J. O. Lundberg, E. Weitzberg, and M. T. Gladwin, "The nitrate-nitrite-nitric oxide pathway in physiology and therapeutics," *Nat. Rev. Drug Discov.* **7**(2), 156–167 (2008).
33. A. P. Castano, T. N. Demidova, and M. R. Hamblin, "Mechanisms in photodynamic therapy: part two–cellular signaling, cell metabolism and modes of cell death," *Photodiagn. Photodyn. Ther.* **2**, 1–23 (2005).
34. A. B. Uzdensky, "Signal transduction and photodynamic therapy," *Curr. Sign. Transd. Ther.* **3**, 55–74 (2008).
35. W. H. Chan, "Photodynamic treatment induces an apoptotic pathway involving calcium, nitric oxide, p53, p21-activated kinase 2, and c-Jun N-terminal kinase and inactivates survival signal in human umbilical vein endothelial cells," *Int. J. Mol. Sci.* **12**, 1041–1059 (2011).
36. L. Zhou and D. Y. Zhu, "Neuronal nitric oxide synthase: structure, subcellular localization, regulation, and clinical implications," *Nitric Oxide* **20**, 223–230 (2009).

Vera D. Kovaleva received her PhD in biophysics in 2016. She is a researcher at the Laboratory of Molecular Neurobiology, Southern

Federal University, Rostov-on-Don, Russia. She is the author of 15 journal papers.

Anatoly B. Uzdensky received his PhD and Dr Sci degrees in biophysics in 1980 and 2005, respectively. He is a professor in biophysics and head of the Laboratory of Molecular Neurobiology, Southern Federal University, Rostov-on-Don, Russia. He is the author of more than 115 journal papers and 3 books. His current research interests include photodynamic therapy, neuroscience, cell biology, and proteomics. He is a member of SPIE, and European, Russian, and American Societies for Photobiology.